Neat1 is a p53-inducible lincRNA essential for transformation suppression

Stephano S. Mello,[1] Carolyn Sinow,[1] Nitin Raj,[1] Pawel K. Mazur,[2] Kathryn Bieging-Rolett,[1] Daniela Kenzelmann Broz,[1] Jamie F. Conklin Imam,[2,3] Hannes Vogel,[4] Laura D. Wood,[5] Julien Sage,[2,3] Tetsuro Hirose,[6] Shinichi Nakagawa,[7] John Rinn,[8] and Laura D. Attardi[1,3]

[1]Department of Radiation Oncology, Stanford University School of Medicine, Stanford, California 94305, USA; [2]Department of Pediatrics, Stanford University School of Medicine, Stanford, California 94305, USA; [3]Department of Genetics, Stanford University School of Medicine, Stanford, California 94305, USA; [4]Department of Pathology, Stanford University School of Medicine, Stanford, California 94305, USA; [5]Department of Pathology, The Sol Goldman Pancreatic Cancer Research Center, The Johns Hopkins University School of Medicine, Baltimore, Maryland 21231, USA; [6]Institute for Genetic Medicine, Hokkaido University, Sapporo 060-0815, Japan; [7]RNA Biology Laboratory, Faculty of Pharmaceutical Sciences, Hokkaido University, Sapporo 060-0812, Japan; [8]Department of Stem Cell and Regenerative Biology, Harvard University, Cambridge, Massachusetts 02138, USA

The *p53* gene is mutated in over half of all cancers, reflecting its critical role as a tumor suppressor. Although p53 is a transcriptional activator that induces myriad target genes, those p53-inducible genes most critical for tumor suppression remain elusive. Here, we leveraged p53 ChIP-seq (chromatin immunoprecipitation [ChIP] combined with high-throughput sequencing) and RNA-seq (RNA sequencing) data sets to identify new p53 target genes, focusing on the noncoding genome. We identify *Neat1*, a noncoding RNA (ncRNA) constituent of paraspeckles, as a p53 target gene broadly induced by mouse and human p53 in different cell types and by diverse stress signals. Using fibroblasts derived from *Neat1*$^{-/-}$ mice, we examined the functional role of *Neat1* in the p53 pathway. We found that *Neat1* is dispensable for cell cycle arrest and apoptosis in response to genotoxic stress. In sharp contrast, *Neat1* plays a crucial role in suppressing transformation in response to oncogenic signals. *Neat1* deficiency enhances transformation in oncogene-expressing fibroblasts and promotes the development of premalignant pancreatic intraepithelial neoplasias (PanINs) and cystic lesions in Kras^{G12D}-expressing mice. *Neat1* loss provokes global changes in gene expression, suggesting a mechanism by which its deficiency promotes neoplasia. Collectively, these findings identify *Neat1* as a p53-regulated large intergenic ncRNA (lincRNA) with a key role in suppressing transformation and cancer initiation, providing fundamental new insight into p53-mediated tumor suppression.

[*Keywords*: p53; lincRNA; *Neat1*; tumor suppression; pancreatic cancer]

Supplemental material is available for this article.

Received May 25, 2016; revised version accepted May 26, 2017.

The role of *p53* as a critical tumor suppressor is well illustrated by the fact that it is found mutated in more than half of all human cancers (Olivier et al. 2010). The highly penetrant cancer predisposition observed in Li-Fraumeni patients with germline mutations in *p53* and in *p53*-null mice further highlights the importance of p53 in tumor suppression (Vousden and Prives 2009; Brady and Attardi 2010). p53 is a cellular stress sensor that responds to signals such as DNA damage and oncogene expression and triggers cell cycle arrest, senescence, or apoptosis to restrain cellular proliferation in the face of these signals. In addition, p53 also regulates other processes, including autophagy and metabolic homeostasis, which may contribute to tumor suppression (Vousden and Prives 2009; Kenzelmann Broz et al. 2013; Kruiswijk et al. 2015).p53 is a transcription factor that drives different biological responses by promoting the expression of a network of target genes. While the target genes involved in promoting cell cycle arrest or apoptosis are well characterized, the target genes responsible for mediating p53 function in tumor suppression remain enigmatic. For example, it has been shown that the target genes critical for DNA damage-induced p53-dependent cell cycle arrest or apoptosis—such as *p21*, *Puma*, and *Noxa*—are dispensable for tumor suppression (Brady et al. 2011; Li et al. 2012; Valente et al. 2013). These findings have raised the question of which p53 target genes are therefore the most essential for suppressing tumorigenesis. Recent genomic approaches, including ChIP-seq (chromatin immunoprecipitation [ChIP] combined with high-throughput sequencing) and RNA-seq (RNA sequencing), have helped to identify new p53-regulated genes whose biological functions in the

Corresponding author: attardi@stanford.edu
Article published online ahead of print. Article and publication date are online at http://www.genesdev.org/cgi/doi/10.1101/gad.284661.116.

p53 tumor suppression pathway could be explored (Kenzelmann Broz et al. 2013; Sánchez et al. 2014; Léveillé et al. 2015; Younger et al. 2015).

Although studies on genes in the p53 network have focused largely on protein-coding genes, in recent years, the role of p53-inducible noncoding RNAs (ncRNAs), including both microRNAs and large intergenic ncRNAs (lincRNAs), in p53 biological responses has been increasingly recognized. The first of these to be discovered, *miR34a*, plays an important role in restricting cellular reprogramming (as does p53) and can promote tumor suppression, by enhancing p53 activity through a positive feedback loop (Krizhanovsky and Lowe 2009; Choi et al. 2011; Okada et al. 2014). Subsequently, several p53-inducible lincRNAs, including *LincRNAp21*, *loc285194, PANDA*, and *DINO*, were identified (Huarte et al. 2010; Hung et al. 2011; Liu et al. 2013; Schmitt and Chang 2016; Schmitt et al. 2016). While these lincRNAs have been shown to regulate cellular proliferation and survival in vitro, cancer phenotypes using mice lacking their cognate genes have not been well explored. Analysis of such p53-regulated lincRNAs in clear genetic model systems in vivo could provide key new insight into p53-mediated tumor suppression.

To identify new ncRNAs regulated by p53 and their functional roles in the p53 pathway, we leveraged ChIP-seq and RNA-seq data sets that we generated previously in wild-type mouse embryonic fibroblasts (MEFs) treated with the DNA-damaging agent doxorubicin to activate p53 (Kenzelmann Broz et al. 2013). We identify the lincRNA *Neat1* as a direct p53 target gene. *NEAT1* was originally identified as an abundant nuclear ncRNA that is an essential component of paraspeckles, nuclear bodies thought to control gene expression through the nuclear retention of hyperedited RNAs (Hutchinson et al. 2007; for review, see Naganuma and Hirose 2013). Here, we interrogated the role of *Neat1* in the p53 pathway using *Neat1* knockout mice. Interestingly, we found that *Neat1* plays an essential role in suppressing both transformation in oncogene-expressing fibroblasts and pancreatic cancer initiation by constraining mutant Kras-induced pancreatic intraepithelial neoplasias (PanINs) and cystic lesions reminiscent of intraductal papillary mucinous neoplasms (IPMNs). Additionally, we found that *Neat1* deficiency in oncogene-expressing fibroblasts is associated with global changes in gene expression. Together, these findings identify *Neat1* as a p53-regulated lincRNA with a fundamental role in suppressing transformation and cancer initiation, providing important new insight into p53-mediated tumor suppression pathways.

Results

Neat1 *is a p53 target gene in various primary and transformed mouse and human cell types*

With the goal of understanding how lincRNAs mediate downstream p53 functions, we used ChIP-seq and RNA-seq data sets that we had generated previously using primary MEFs treated with doxorubicin to identify key lincRNAs induced by p53 (Fig. 1A; Kenzelmann Broz et al. 2013). Of the 432 genes that we delineated as bound and modulated by p53, we identified two ncRNAs, *Neat1* and *Gm5801*, although only *Neat1* was significantly induced by p53, while *Gm5801* was weakly repressed by p53. We found a clear p53-binding peak 1.3 kb upstream of the *Neat1* transcription start site, which contained a consensus p53-binding element and to which we could confirm p53 binding by ChIP-qPCR (ChIP combined with quantitative PCR [qPCR] (Fig. 1B). To validate that *Neat1* expression is activated by p53 in mouse cells, we performed qRT–PCR analysis of wild-type and $p53^{-/-}$ MEFs treated with doxorubicin and found that, indeed, *Neat1* is activated by doxorubicin in a p53-dependent manner (Fig. 1C). *Neat1* was also induced in a p53-dependent manner by UV-C radiation, another DNA-damaging agent that activates p53, but through a different mechanism (Fig. 1C). Finally, to determine whether p53 regulates *Neat1* in other cell types, we examined *Neat1* expression in doxorubicin-treated wild-type and $p53^{-/-}$ mouse embryonic stem cells (ESCs) and found largely p53-dependent induction by doxorubicin (Fig. 1D). Collectively, these findings confirm that *Neat1* is bound and regulated by mouse p53 in multiple settings. These data are consistent with published reports showing that human p53 binds to the *NEAT1* locus and activates its expression in human fibroblasts and cancer cell lines (Botcheva et al. 2011; Blume et al. 2015; Adriaens et al. 2016).

Our own analyses bolstered the identity of *NEAT1* as a p53 target gene in human cells. We also identified one strongly enriched p53 peak in our human fibroblast p53 ChIP-seq data, located 1.4 kb upstream of the transcriptional start site of *NEAT1*. p53 binding occurs in a position analogous to the peak found in mouse *Neat1*, and we found that this region harbored a site with a near-perfect match to the consensus p53-binding site (Fig. 1E; Younger et al. 2015). Moreover, we found that both the long (*NEAT1_2*, 23 kb) and short (*NEAT1_1*, 3.7 kb) isoforms of *NEAT1* as well as *NEAT1* paraspeckles are induced by doxorubicin in primary human fibroblasts and human ESCs in a p53-dependent manner (Fig. 1F–H; Supplemental. Fig. S1A,B). Furthermore, treatment of human ESCs and A549 lung cancer cells with Nutlin-3a, a p53 stabilizer that does not rely on DNA damage (Vassilev et al. 2004), showed that *NEAT1* is induced by p53 in the absence of genotoxic stress (Fig. 1H,I). Finally, treatment of wild-type and *p53*-null HCT116 colorectal carcinoma cells treated with doxorubicin revealed that expression of both *NEAT1* isoforms is doxorubicin-inducible and that this response depends on p53 (Fig. 1J,K). Together, these findings underscore a conserved induction of *NEAT1* in response to various p53-activating signals in a diversity of mouse and human cell types, raising the possibility that *NEAT1* may play an important role in p53 responses.

Neat1 *is dispensable for p53-dependent DNA damage responses*

We next sought to elucidate the role of *Neat1* in the p53 pathway. To unequivocally establish the contribution of

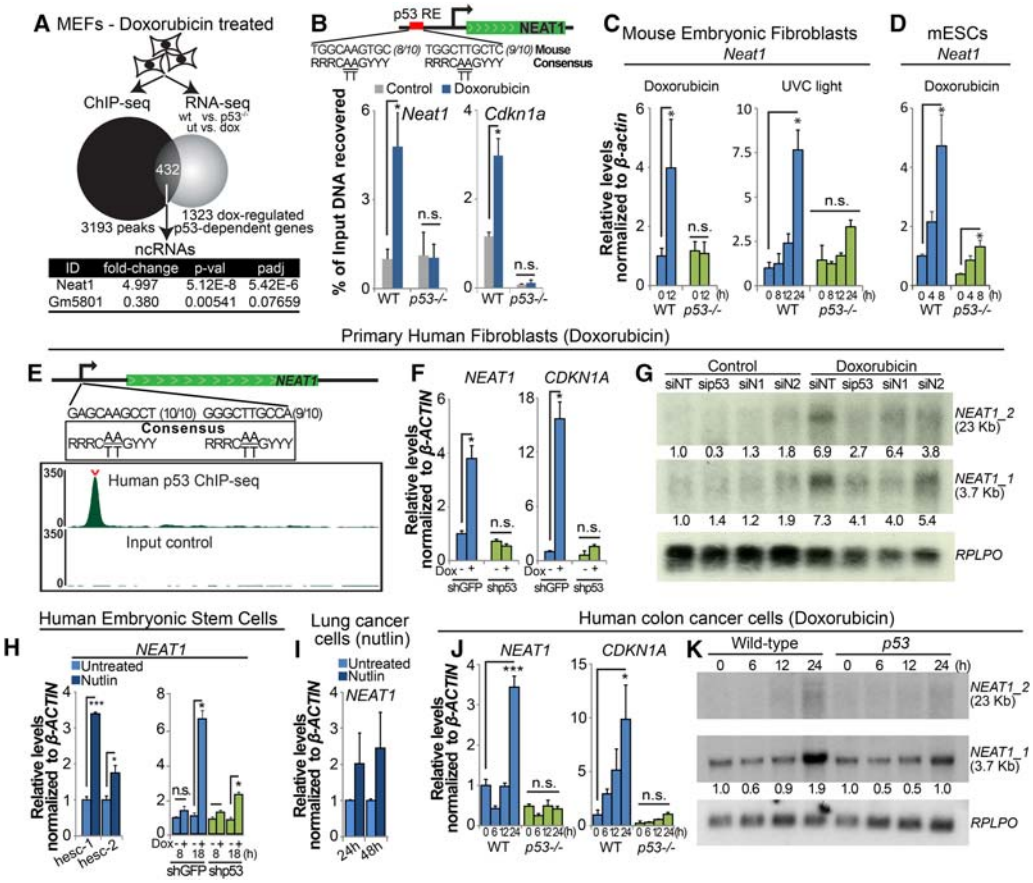

Figure 1. *Neat1* is a p53 target gene in mouse and human cells. (*A*) Experimental outline that led to the discovery of *Neat1* as a p53 target gene. Wild-type and $p53^{-/-}$ MEFs were either left untreated or treated with 0.2 µg/mL doxorubicin for 6 h to generate a list of doxorubicin-regulated p53-dependent RNAs using RNA-seq. Wild-type MEFs were also treated with doxorubicin for 6 h prior to ChIP-seq analysis (Kenzelmann-Broz et al. 2013). Four-hundred-thirty-two genes bound and regulated by p53 were defined, and the annotation of long ncRNAs among these pinpointed *Neat1* as a novel p53-inducible target gene. (*B*) ChIP-qPCR testing for p53 binding at a peak identified in *Neat1* by ChIP-seq analysis together with *Cdkn1a* as a positive control. The percentage of immunoprecipitated DNA relative to input is indicated. $p53^{-/-}$ MEFs served as a negative control. (*C*) qRT–PCR analysis of *Neat1* expression in wild-type and $p53^{-/-}$ MEFs treated with 0.2 µg/mL doxorubicin (*left*) or 20 J/m^2 UV light (*right*) and collected at the indicated time points, normalized to β-*actin*. (*D*) qRT–PCR analysis of *Neat1* expression in mouse ESCs treated with 0.2 µg/mL doxorubicin for the indicated times, normalized to β-*actin*. (*E*) Human p53 ChIP-seq profiles (Younger et al. 2015) in primary human fibroblasts reveal a strong p53-binding site in the promoter of *NEAT1*. The *top* track shows the p53 ChIP sample, with the carat indicating the "called" peak as determined by DNANexus. The *bottom* track shows ChIP-seq input reads. The numbers in parentheses indicate the numbers of base pairs in individual half-sites matching the consensus sequence. (*F*) qRT–PCR analysis of *NEAT1* and *CDKN1A* in primary human fibroblasts expressing shGFP or shp53 8 h after initiating doxorubicin treatment, normalized to β-*ACTIN*. (*G*) Northern blot of doxorubicin-treated (for 24 h) primary human fibroblasts transfected with a scrambled siRNA (siNT), sip53, or either of two different siRNAs against *NEAT1* (siN1 and siN2). The numbers *below* the blots correspond to the expression levels normalized to the *RPLPO* loading control. (*H*, *left*) *NEAT1* expression levels by qRT–PCR in two different human ESCs treated with Nutlin3a for 2 d, normalized to β-*ACTIN*. (*Right*) *NEAT1* expression levels by qRT–PCR in human ESCs expressing shGFP or shp53 and left untreated or treated with doxorubicin for the indicated times, normalized to β-*ACTIN*. (*I*) *NEAT1* expression levels by qRT–PCR in human A549 lung cancer cells treated with Nutlin3a for 1 or 2 d, normalized to β-*ACTIN*. (*J*) qRT–PCR analysis of *NEAT1* and *CDKN1A* in wild-type and *p53*-null HCT116 cells treated with 0.2 µg/mL doxorubicin for different times, normalized to β-*ACTIN*. (*K*) Northern blot of wild-type and *p53*-null HCT116 cells after doxorubicin treatment for different lengths of time. *RPLPO* serves as a loading control. The numbers *below* the blots correspond to the expression levels normalized to *RPLPO*. Error bars represent ±SD. (*) $P \leq 0.05$; (***) $P \leq 0.001$; (n.s.) nonsignificant, based on the two-tailed unpaired Student's *t*-test.

Neat1 to p53 function, we used *Neat1* knockout mice (Nakagawa et al. 2011). Notably, while MEFs derived from wild-type mice are completely proficient in forming paraspeckles in the nucleus, no paraspeckles are observed in $Neat1^{-/-}$ MEFs, as seen by costaining for *Neat1* and the paraspeckle protein Sfpq (Fig. 2A). We first focused on p53 responses to acute genotoxic stress, upon which p53 directs either cell cycle arrest or apoptosis. To assess whether *Neat1* is necessary for p53-dependent DNA damage responses, we exposed primary MEFs derived from wild-type, $p53^{-/-}$, and $Neat1^{-/-}$ mice to 5 Gy of ionizing radiation, a classical assay to test for p53-dependent G1 cell

cycle arrest. We then evaluated the cell cycle profiles 18 h after irradiation. In these assays, we observed that both wild-type and *Neat1*$^{-/-}$ MEFs underwent G1 cell cycle arrest to an equivalent extent, while the *p53*$^{-/-}$ MEFs failed to undergo G1 arrest, suggesting that *Neat1* is dispensable for p53-dependent cell cycle arrest (Fig. 2B).

The expression of the E1A and HRasV12 oncogenes sensitizes MEFs to apoptosis in response to DNA damage (Lowe et al. 1993). Thus, to test whether *Neat1* plays a role in p53-dependent apoptosis, we treated *E1A;HRasV12*-expressing wild-type, *p53*$^{-/-}$, and *Neat1*$^{-/-}$ MEFs with doxorubicin and evaluated apoptosis using Annexin V/propidium iodide (PI) staining 12 and 24 h later. Consistent with known p53 biology, *E1A;HRasV12*-expressing wild-type MEFs efficiently underwent apoptosis, while the *E1A;HRasV12*-expressing *p53*$^{-/-}$ MEFs remained resistant to apoptosis (Fig. 2C). The levels of apoptosis in *E1A;HRasV12*-expressing *Neat1*$^{-/-}$ MEFs were not statistically significantly different from those in *E1A;HRasV12*-expressing wild-type MEFs, indicating that *Neat1* is dispensable for p53-dependent apoptosis. Together, these experiments suggest that, although *Neat1* is induced by DNA damage, *Neat1* is not necessary for the p53-dependent DNA damage responses of cell cycle arrest and apoptosis, at least in the cellular contexts examined.

Neat1 *suppresses transformation in oncogene-expressing fibroblasts*

Given that *Neat1* is dispensable for p53 responses to genotoxic stress and that recent studies have suggested that distinct transcriptional programs are required for p53 action downstream from acute DNA damage and oncogenic signals (Brady et al. 2011; Bieging et al. 2014), we next sought to establish whether *Neat1* might instead be important for p53 responses to oncogenic signals. Specifically, we examined the contribution of *Neat1* to transformation suppression in a classic oncogene-expressing fibroblast model. We first investigated whether *Neat1* deficiency can increase transformation by comparing *E1A;HRasV12*-expressing wild-type, *p53*$^{-/-}$, and *Neat1*$^{-/-}$ MEFs. Importantly, *Neat1* deficiency also compromises paraspeckle formation in this context, as determined by *Neat1*/Sfpq costaining (Fig. 3A). We confirmed next that p53 deficiency greatly enhances both clonogenic potential in low-density plating assays and anchorage-independent growth in soft agar assays relative to p53-expressing cells, as reported (Kenzelmann Broz et al. 2013). Interestingly, we found that *Neat1* deficiency also significantly increases both clonogenic potential and anchorage-independent growth relative to *Neat1*-proficient cells (Fig.

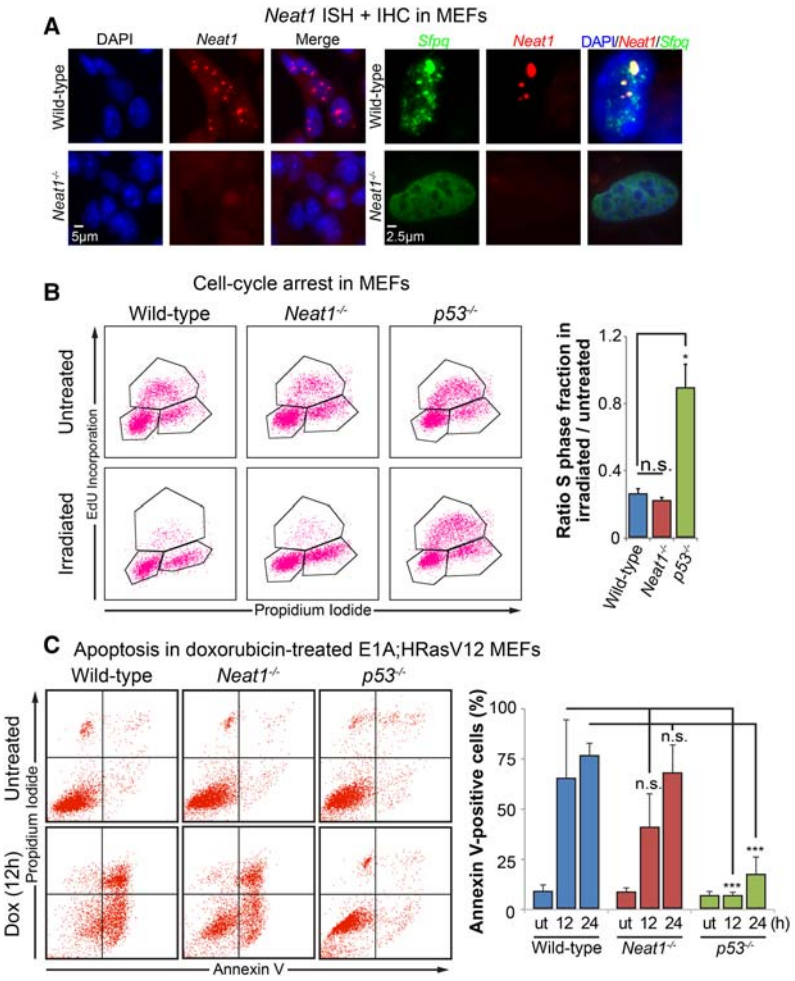

Figure 2. *Neat1* is dispensable for p53 acute DNA damage responses. (*A*, *left*) RNA-FISH using a Quasar 570-labeled complex probe against *Neat1* to examine paraspeckles in wild-type and *Neat1*$^{-/-}$ primary MEFs. Nuclei were stained with DAPI. (*Right*) High-magnification detail of RNA-FISH against *Neat1* (using a Quasar 570-labeled probe) and immunostaining of the paraspeckle protein *Sfpq* in wild-type and *Neat1*$^{-/-}$ primary MEFs. Nuclei were stained with DAPI. (*B*) Cell cycle arrest analysis in MEFs of different genotypes. (*Left*) Representative FACS analyses of 5-ethynyl-2 deoxyuridine (EdU)-incorporating and propidium iodide (PI)-stained untreated and irradiated (5 Gy) MEFs of different genotypes. (*Right*) Quantification of G1 arrest response in MEFs, indicated by the ratio of the S-phase fraction in irradiated cells to the S-phase fraction in untreated cells. $n = 3$. (*C*) Apoptosis analysis in MEFs of different genotypes. (*Left*) Representative FACS analyses of Annexin V and PI staining in *E1A;HRasV12* MEFs of each genotype. (*Right*) Quantification of Annexin V-positive *E1A;HRasV12* MEFs of different genotypes (wild type, *Neat1*$^{-/-}$, and *p53*$^{-/-}$) after being either left untreated (ut) or treated with 0.2 μg/mL doxorubicin for 12 or 24 h. $n = 6$. At least two different MEF lines were used in these experiments. Error bars represent ±SD. (*) $P \leq 0.05$; (***) $P \leq 0.001$; (n.s.) nonsignificant, based on the two-tailed unpaired Student's *t*-test.

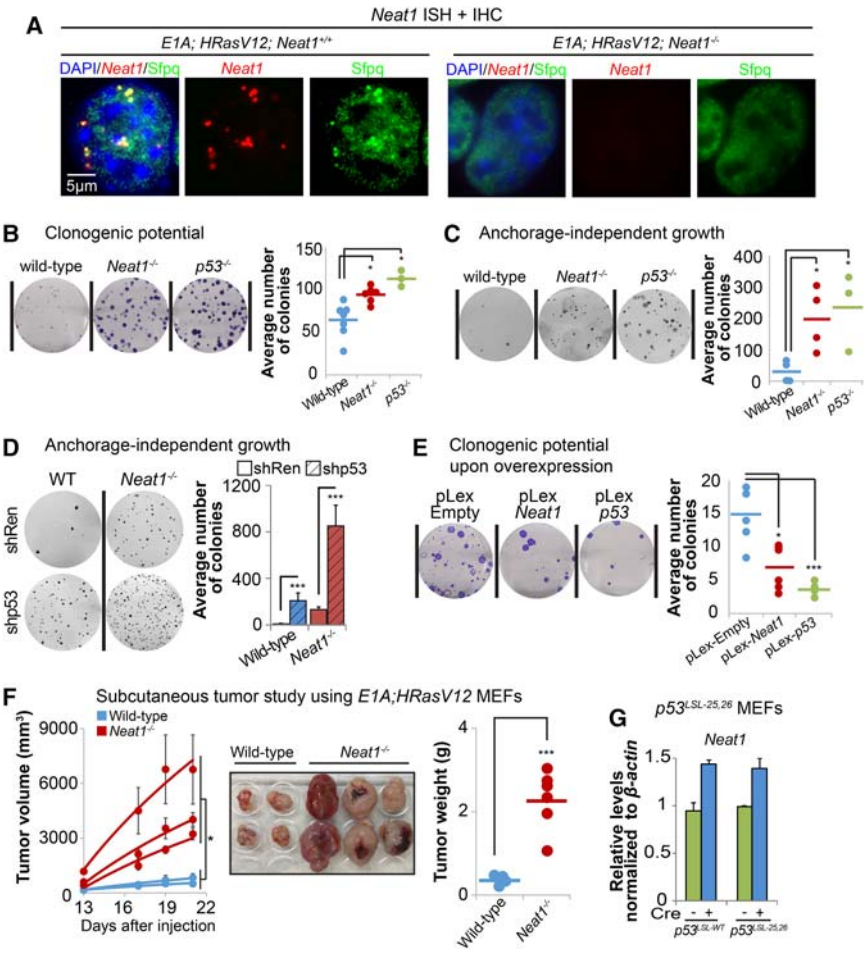

Figure 3. *Neat1* suppresses transformation in oncogene-expressing MEFs. (*A*) RNA-FISH against *Neat1* (using a Quasar 570-labeled probe) and immunostaining of the paraspeckle protein *Sfpq* in *E1A; HRasV12* and *E1A;HRasV12;Neat1*$^{-/-}$ MEFs. Nuclei were stained with DAPI. (*B*) Clonogenic potential of *E1A;HRasV12* MEFs of different genotypes (wild type, *Neat1*$^{-/-}$, and *p53*$^{-/-}$) assayed using a low-density plating assay. Colonies were stained with crystal violet. (*Left*) Representative wells from clonogenic assays are shown. (*Right*) Dots represent average colony numbers from triplicate samples, integrating results from three different experiments using two to four different MEF lines per genotype. (*C*) Anchorage-independent growth of *E1A;HRasV12* MEFs of different genotypes (wild type, *Neat1*$^{-/-}$, and *p53*$^{-/-}$) in a soft agar colony assay. Colonies were stained with Giemsa. (*Left*) Representative wells are shown. (*Right*) Dots represent average colony numbers from triplicate samples. Two independent experiments using two to four MEF lines per genotype were performed. (*D*) Anchorage-independent growth of *E1A;HRasV12* MEFs of different genotypes (wild type and *Neat1*$^{-/-}$) upon the introduction of control shRNA or shRNA against p53. Colonies were stained with Giemsa. (*Left*) Representative wells are shown. (*Right*) Dots represent average colony numbers for triplicate samples from two independent experiments using two MEF lines per genotype. (*E*) Clonogenic potential of *E1A;HRasV12; p53*$^{-/-}$ MEFs after *Neat1* or p53 overexpression. pLex-empty served as a negative control. (*Left*) Representative wells from clonogenic assays are shown. (*Right*) Dots represent average colony number for triplicate samples from two independent experiments. Independent experiments for *B–E* were performed with both different MEF lines and some MEF lines multiple times to ensure both repetition and representation by multiple MEF lines. (*F, left*) Average tumor volumes as a function of time in *Scid* mice injected with *E1A;HRasV12*-expressing wild-type and *Neat1*$^{-/-}$ MEFs. The dots represent the average of tumors from the left and right flanks of a given animal. Two different *E1A;HRasV12; Neat1*$^{+/+}$ and three different *E1A;HRasV12;Neat1*$^{-/-}$ MEF lines were used, totaling four and six tumors of each genotype, respectively. (*Middle*) Images of the tumors at the end of the experiment, 22 d after injection. (*Right*) Tumor weight at day 22. (*G*) *Neat1* expression levels by qRT–PCR in homozygous *p53*$^{LSL\text{-}wt}$ and *p53*$^{LSL\text{-}25,26}$ primary MEFs upon adeno-Cre-induced reactivation of p53, normalized to β-*actin*. Error bars represent ±SD. (*) $P \leq 0.05$; (***) $P \leq 0.001$, based on the two-tailed unpaired Student's *t*-test.

3B,C), indicating that *Neat1* loss promotes transformation similarly to p53 deficiency. To query whether *Neat1* is the main conduit for p53-mediated transformation suppression, we attenuated *p53* expression by knockdown in *E1A;HRasV12*-expressing wild-type and *Neat1*$^{-/-}$ MEFs. We observed an increase in anchorage-independent growth upon *p53* knockdown in *E1A;HRasV12;Neat1*$^{-/-}$ MEFs, suggesting that *Neat1* is simply one component downstream from p53 in tumor suppression (Fig. 3D). This finding is consistent with our observation that overexpression of the short isoform of *Neat1* (*Neat1_1*) is sufficient to inhibit transformation in the absence of p53 but not as potently as p53 (Fig. 3E; Supplemental Fig. S2). Finally, to interrogate *Neat1* tumor suppressor activity in vivo, we injected *E1A;HRasV12;wild-type* and *E1A; HRasV12;Neat1*$^{-/-}$ cells subcutaneously into immunocompromised mice. In concordance with our observations in vitro, *Neat1* deficiency resulted in an increase in tumor mass and volume (Fig. 3F), indicating that *Neat1* also has tumor suppressor activity in vivo. This finding is consistent with the p53^{25,26} transactivation domain 1 mutant that we generated previously (which activates only a subset of p53 target genes and yet serves as a potent tumor suppressor) being able to activate *Neat1* (Fig. 3G; Brady et al. 2011). Collectively, these findings show that *Neat1* plays a key role in suppressing transformation of oncogene-expressing fibroblasts, as does p53.

Neat1 *suppresses transformation in pancreatic cancer cells*

As cancers derived from epithelia or carcinomas represent the majority of human cancers, we next sought to

examine the role for *Neat1* in a carcinoma model. We focused specifically on pancreatic ductal adenocarcinoma (PDAC), which can be modeled in mice by *Pdx1*-Cre-mediated expression of activated $Kras^{G12D}$ in the pancreas, as we discovered that *Neat1* expression is also p53-dependent in $Kras^{G12D}$-expressing premalignant pancreatic epithelium in an RNA-seq data set that we generated (Fig. 4A; SS Mello, LJ Valente, N Raj, JA Seoane, BM Flowers, J McClendon, KT Bieging-Rolett, J Lee, D Ivanochko, MM Kozak, et al., in prep.). Based on this observation, we hypothesized that *Neat1* could be involved in p53-dependent PDAC suppression. To test this idea, we assessed whether *Neat1* overexpression could also reduce the tumorigenicity of *p53*-null pancreatic cancer cells using a clonogenic potential assay. Indeed, we found that, as with p53, overexpression of *Neat1* in a $p53^{-/-}$ pancreatic cancer cell line decreased clonogenic potential, and this was associated with an increase in paraspeckles (Fig. 4B, C; Supplemental Fig. S3). These data indicate that ectopic *Neat1* expression can suppress transformation in different cell types.

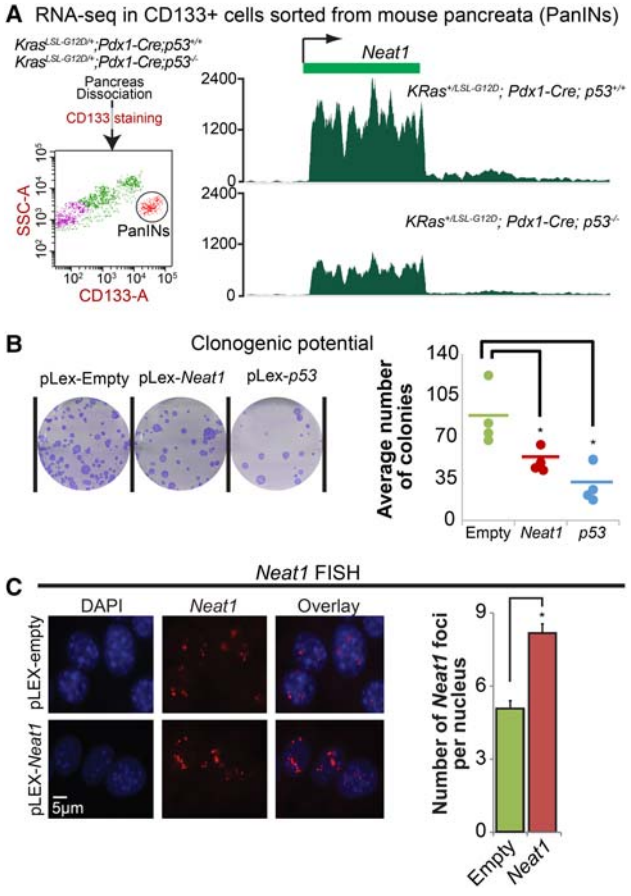

Figure 4. *Neat1* is associated with suppression of pancreatic cancer cell growth. (*A*) Tracks representing *Neat1* expression levels in RNA-seq data from $CD133^+$ FACS-sorted mouse pancreata from $KRas^{+/LSL\text{-}G12D}$;*Pdx1-Cre*;$p53^{+/+}$ mice (*top*) and $KRas^{+/LSL\text{-}G12D}$;*Pdx1-Cre*;$p53^{-/-}$ mice (*bottom*). (*B*) Clonogenic potential of a PDAC cell line derived from $KRas^{G12D}$;*Pdx1-Cre*;$p53^{fl/fl}$ mice after *Neat1* or p53 overexpression. pLex-empty served as a negative control. (*Left*) Representative wells from clonogenic assays are shown. (*Right*) Dots indicate average colony number of triplicates from each independent experiment. $n = 4$. (*) $P < 0.05$, based on the two-tailed unpaired Student's *t*-test. (*C*) RNA-FISH for *Neat1* in *p53*-null PDAC cells after empty vector or *Neat1* transduction. (*Left*) Representative RNA-FISH images for *Neat1*. Nuclei were stained with DAPI. (*Right*) Average number of *Neat1* foci ± SEM per nucleus. (*) $P \leq 0.05$, based on the two-tailed unpaired Student's *t*-test.

Neat1 *deficiency promotes pancreatic cancer initiation*

p53 is known to serve as a barrier to PDAC development in $KRas^{+/LSL\text{-}G12D}$ mice expressing Cre recombinase under the control of a pancreatic-specific promoter. Given our initial data highlighting the capacity of *Neat1* to suppress transformation of pancreatic cancer cells, we sought to determine whether *Neat1* can restrain pancreatic cancer initiation in vivo. As RNA-FISH in pancreas tissue showed that the numbers of *Neat1* paraspeckles in $KRas^{+/LSL\text{-}G12D}$;*Ptf1a-Cre*;$Neat1^{+/-}$ mice are significantly lower than in $KRas^{+/LSL\text{-}G12D}$;*Ptf1a-Cre*;$Neat1^{+/+}$ mice (Fig. 5A), we used both *Neat1* heterozygous and *Neat1*-null mice to determine the role of *Neat1* in suppression of pancreatic cancer initiation. Pancreatic cancer can arise through the dedifferentiation of pancreatic acinar cells into ductal-like cells, a process known as acinar-to-ductal metaplasia (ADM), leading to premalignant lesions known as PanINs, which ultimately progress to PDAC (Guerra et al. 2007; Zhu et al. 2007; Morris et al. 2010; Kopp et al. 2012). PDAC has also been reported to arise from cystic lesions known as IPMNs, which are thought to originate from ductal cells (Matthaei et al. 2011; von Figura et al. 2014).

We first examined the consequences of *Neat1* deficiency for ADM and PanIN formation in $KRas^{+/LSL\text{-}G12D}$; *Ptf1a-Cre* mice treated with cerulein, an inducer of pancreatitis that enhances pancreatic cancer initiation by triggering ADM and PanIN formation (Guerra et al. 2011). Interestingly, we found that both $KRas^{+/LSL\text{-}G12D}$; *Ptf1a-Cre*;$Neat1^{+/-}$ and $KRas^{+/LSL\text{-}G12D}$;*Ptf1a-Cre*;$Neat1^{-/-}$ mouse pancreata displayed dramatic ADM (with a great increase in PanIN burden marked by Muc5ac or Alcian blue positivity) relative to $KRas^{+/LSL\text{-}G12D}$;*Ptf1a-Cre*; wild-type mouse pancreata (Fig. 5B). These findings underscore a critical function for *Neat1* in suppressing pancreatic cancer initiation. The increased propensity for ADM observed with *Neat1* deficiency was further supported by an ex vivo ADM transdifferentiation assay using organoid cultures of acini from $Kras^{LSL\text{-}G12D}$;$Neat1^{+/+}$ and $Kras^{LSL\text{-}G12D}$;$Neat1^{-/-}$ mice (Supplemental Fig. S4). In addition to increasing ADM, *Neat1* deficiency also increased PanIN burden by enhancing the percentage of Ki67-positive cells in PanINs relative to *Neat1*-expressing PanINs, suggesting that *Neat1* also restricts proliferation in PanINs (Fig. 5B). Interestingly, we also observed that both heterozygous and homozygous loss of *Neat1* led to the increased formation of cystic lesions lined by mucinous epithelium, some of which were low-grade, while others had clear papillae, histologically similar to human

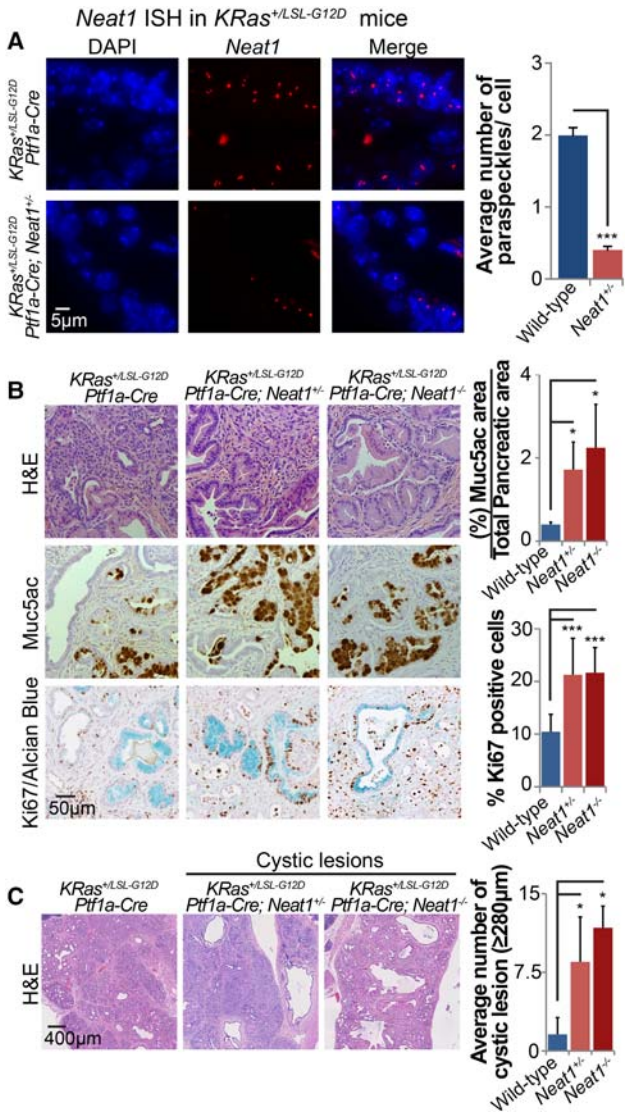

Figure 5. *Neat1* suppresses pancreatic cancer initiation in vivo upon pancreatitis. (*A*) RNA-FISH for *Neat1* in pancreas sections of cerulein-treated $KRas^{+/LSL\text{-}G12D}$;*Ptf1a-Cre*;$Neat1^{+/+}$ and $KRas^{+/LSL\text{-}G12D}$;*Ptf1a-Cre*;$Neat1^{+/-}$ mice. (*Left*) Representative RNA-FISH images for *Neat1*. Nuclei were stained with DAPI. (*Right*) Average *Neat1* foci ± SD per nucleus (*B*) Pancreas histology of $KRas^{+/LSL\text{-}G12D}$;*Ptf1a-Cre*;$Neat1^{+/+}$ ($n = 13$), $Kras^{+/LSL\text{-}G12D}$;*Ptf1a-Cre*;$Neat1^{+/-}$ ($n = 6$), and $Kras^{+/LSL\text{-}G12D}$;*Ptf1a-Cre*;$Neat1^{-/-}$ ($n = 4$) mice with acute pancreatitis 7 d after cerulein treatment. (*Left*) Representative hematoxylin and eosin (H&E), Muc5ac (PanIN marker), and Ki67/Alcian blue costaining (markers of proliferation and PanINs, respectively) of pancreata from cerulein-treated cohorts. (*Top right*) Average PanIN area ± SD as a percentage of total pancreas area, as determined by Muc5ac quantification. (*Bottom right*) Average percentage ± SD of proliferating PanIN cells per mouse pancreas, as determined by the counting of at least 1000 Alcian blue cells. (*C*, *left*) Representative low-magnification H&E staining of pancreata from cerulein-treated cohorts, evidencing large cystic lesions reminiscent of human IPMN lesions. (*Right*) Average number of cystic lesions per mouse ± SD. Cystic lesions are defined by size criteria (diameter ≥280 μm). (*) $P \leq 0.05$; (***) $P \leq 0.001$, based on the two-tailed unpaired Student's *t*-test.

IPMNs presenting gastric-type differentiation (Fig. 5C; Supplemental Figs. S5, S7). Together, these findings suggest that *Neat1* loss enhances the formation of multiple types of preneoplastic lesions in the context of Kras activation and pancreatitis.

To analyze the role of *Neat1* in maintaining pancreatic homeostasis in aging mice, we next explored whether *Neat1* deficiency promotes spontaneous ADM and PanIN formation or the generation of IPMN-like lesions in the absence of pancreatitis. We aged $KRas^{+/LSL\text{-}G12D}$;*Ptf1a-Cre*;$Neat1^{+/+}$, $KRas^{+/LSL\text{-}G12D}$;*Ptf1a-Cre*;$Neat1^{+/-}$, and $KRas^{+/LSL\text{-}G12D}$;*Ptf1a-Cre*;$Neat1^{-/-}$ mice for 5 mo and found that *Neat1*-deficient mice presented a dramatic loss of normal acinar parenchyma and an accumulation of PanIN lesions relative to $KRas^{+/LSL\text{-}G12D}$;*Ptf1a-Cre*;$Neat1^{+/+}$ mice, as indicated by hematoxylin and eosin (H&E) staining and diminished expression of the acinar marker amylase accompanied by positivity for the ductal marker Ck19 (Fig. 6A). Similar to what we observed in cerulein-treated mice at early time points, we found that the loss of *Neat1* also increased the percentage of Ki67-positive cells in Ck19-positive lesions of aging mice (Fig. 6B). Interestingly, we again observed a significant increase in mucinous cystic lesions in aging $KRas^{+/LSL\text{-}G12D}$;*Ptf1a-Cre*;$Neat1^{+/-}$ and $KRas^{+/LSL\text{-}G12D}$;*Ptf1a-Cre*;$Neat1^{-/-}$ mice compared with $KRas^{+/LSL\text{-}G12D}$;*Ptf1a-Cre*;$Neat1^{+/+}$ mice (Fig. 6C; Supplemental Figs. S6, S7). While *Neat1* deficiency enhanced the formation of both PanIN and IPMN-like preneoplastic lesions (Fig 6), there was no increased cancer predisposition at this time point, suggesting that *Neat1* loss promotes efficient ADM and cystic lesion/IPMN formation but that it may take more time or potentially cooperating genetic lesions to fully develop cancer. Together, these findings suggest that *Neat1* suppresses the development of pancreatic neoplasias in vivo and does so by restricting ADM, limiting PanIN proliferation, and suppressing the development of cystic lesions.

Neat1 *deficiency induces global gene expression profile changes*

To gain insight into how *Neat1* loss might promote both transformation and the development of preneoplastic lesions, we leveraged our tractable in vitro E1A;HRasV12 cell model to analyze genome-wide expression profiles in the presence and absence of *Neat1* by RNA-seq. Comparison of gene expression profiles in four *E1A;HRasV12;*$Neat1^{+/+}$ and four *E1A;HRasV12;*$Neat1^{-/-}$ MEF lines revealed that loss of *Neat1* results in significant expression level changes in ~1300 genes (*q*-value 0.005) (Fig. 7A). Analysis using Enrichr (Chen et al. 2013; Kuleshov et al. 2016) revealed that most up-regulated genes were related to mechanisms of protein synthesis (data not shown), a process that is commonly enhanced during tumorigenesis (Truitt and Ruggero 2016). Enrichr also identified gene expression programs down-regulated upon *Neat1* loss in *E1A;HRasV12*-expressing cells, including nervous system development and function and axon guidance programs, which have been associated previously with cancer development (Fig. 7B,C; Dallol et al. 2003; Chedotal et al. 2005;

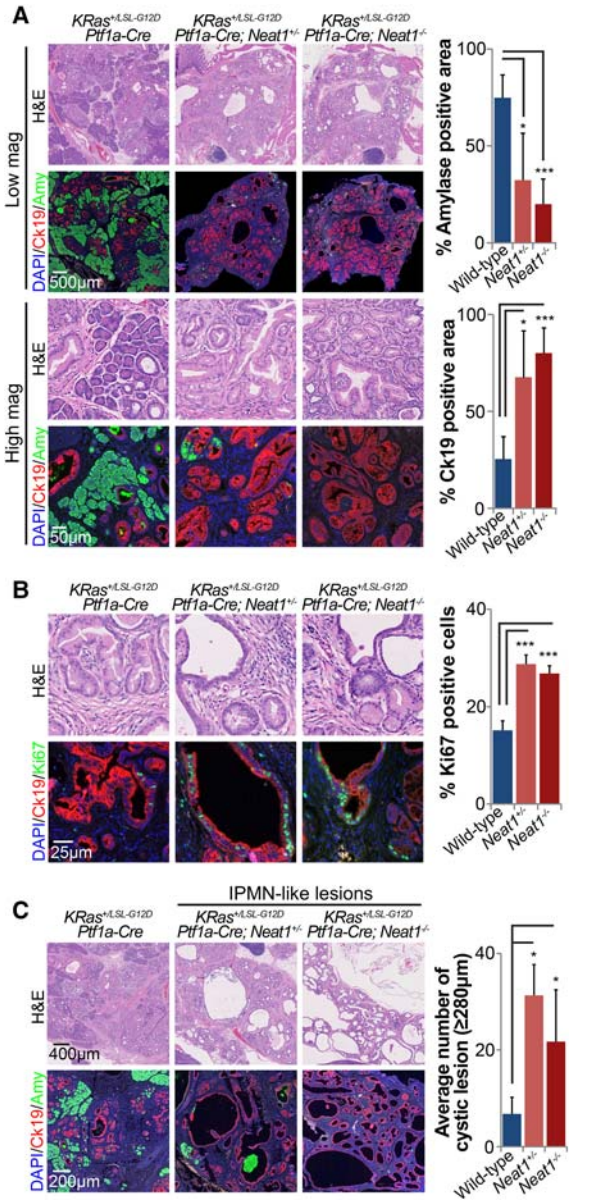

Figure 6. *Neat1* suppresses pancreatic cancer initiation in vivo in aging mice. (*A*) Pancreas histology of 5-mo-old $KRas^{+/LSL\text{-}G12D}$; $Ptf1a\text{-}Cre;Neat1^{+/+}$ ($n = 5$), $Kras^{+/LSL\text{-}G12D}$;$Ptf1a\text{-}Cre;Neat1^{+/-}$ ($n = 3$), and $Kras^{+/LSL\text{-}G12D}$;$Ptf1a\text{-}Cre;Neat1^{-/-}$ ($n = 4$) mice. (*Left*) Representative H&E, amylase + Ck19 double-immunofluorescence staining (specific markers of acinar cells and epithelial cells of ductal origin, respectively) of pancreata from aged cohorts. (*Right*) Average amylase and Ck19-positive areas ± SD as a percentage of total pancreas area. (*B*, *left*) Representative H&E and Ck19 + Ki67 staining (markers of epithelial lesions and proliferation, respectively) of pancreata from aged cohorts. (*Right*) Percentage ± SD of proliferating Ck19-positive epithelial cells, as determined by counting at least 1000 cells. (*C*, *left*) Representative low-magnification H&E staining and amylase + Ck19 double-immunofluorescence staining of pancreata from aged cohorts, evidencing large cystic lesions reminiscent of human IPMN lesions. (*Right*) Average number of cystic lesions per mouse ± SD. Cystic lesions are defined by size criteria (diameter ≥280 μm) ± SD. (*) $P \leq 0.05$; (***) $P \leq 0.001$, based on the two-tailed unpaired Student's *t*-test.

Biankin et al. 2012; Mi Je et al. 2013; Göhrig et al. 2014). We confirmed the differential expression of various genes in these categories by qRT–PCR analysis in *E1A;HRasV12;wild-type* and *E1A;HRasV12;*$Neat1^{-/-}$ MEF lines, focusing on genes such as *Srgap3*, *Dll1*, *Reln*, and *Plxna4*, which have been shown previously to display tumor suppressor activity (Sato et al. 2006; Balakrishnan et al. 2009; Zhang et al. 2011; Castellano et al. 2016). Moreover, given that deficiency in SWI/SNF complex function leads to the formation of IPMNs in mouse models for PDAC (von Figura et al. 2014; Roy et al. 2015), we also queried the status of chromatin remodeling gene expression in *E1A;HRasV12;*$Neat1^{-/-}$ MEFs using the RNA-seq data. Interestingly, we found that expression of various SWI/SNF components, such as *Smarca1* and *Smarcc2*, was reduced in *Neat1*-deficient cells relative to controls (Fig. 7C,D). Importantly, the SWI/SNF complex, including the *Smarca1* and *Smarcc2* subunits, has been shown to have an extensive role in tumor suppression (Weissman and Knudsen 2009; Wilson and Roberts 2011; Amankwah et al. 2013; Takeshima et al. 2015). Additionally, we found that *Ogt*, a chromatin modifier involved in histone GlcNAcylation, is down-regulated in $Neat1^{-/-}$ cells. To determine whether this compromise in gene expression could also explain the pancreatic phenotypes that we observed, we examined the expression of some of these genes in *Neat1*-deficient pancreata. Interestingly, many, but not all, of these genes display diminished expression with *Neat1* loss in the pancreas, suggesting that these gene expression changes could underlie the phenotypes seen in *Neat1*-deficient pancreata (Fig. 7E).

The enhanced formation of ADMs, PanINs, and mucinous cystic lesions in $KRas^{G12D}$-expressing *Neat1*-deficient mice suggests that these mice are more susceptible to the dedifferentiation process that precedes the generation of preneoplastic lesions. To investigate whether *Neat1* has a role in inhibiting dedifferentiation, we used gene set enrichment analysis (GSEA) to analyze our MEF RNA-seq data and test whether *Neat1* deficiency impacts the expression of genes involved in pancreas development. We generated a GSEA signature gene set based on a previously published compilation of gene regulatory networks involved in pancreas development and differentiation (Arda et al. 2013). We found that the expression of various pancreas development genes, such as *Dll1*, *Gata6*, *Bhlha15*, *Mist1*, *Foxa1*, and *Neurod1*, is decreased in *E1A;HRasV12;*$Neat1^{-/-}$ cells relative to *E1A;HRasV12;*$Neat1^{+/+}$ MEFs (Fig. 7F). Furthermore, we found that a subset of these genes—*Bhlha15* and *Sox9*—is also down-regulated in *Neat1*-deficient pancreata (Fig. 7G). Interestingly, *Bhlha15* has a key role in pancreas development, as it is necessary for acinar cell differentiation and maintenance of the exocrine pancreas (Shi et al. 2009; Direnzo et al. 2012; Martinelli et al. 2013). Moreover, Sox9, known as a master regulator of the pancreatic developmental program, is responsible for maintaining the embryonic and adult ductal state (Seymour 2014), and a decrease in Sox9-positive cells was associated previously with mucinous cystic lesions (Tanaka et al. 2013). These findings suggest that *Neat1* deficiency impacts the regulatory

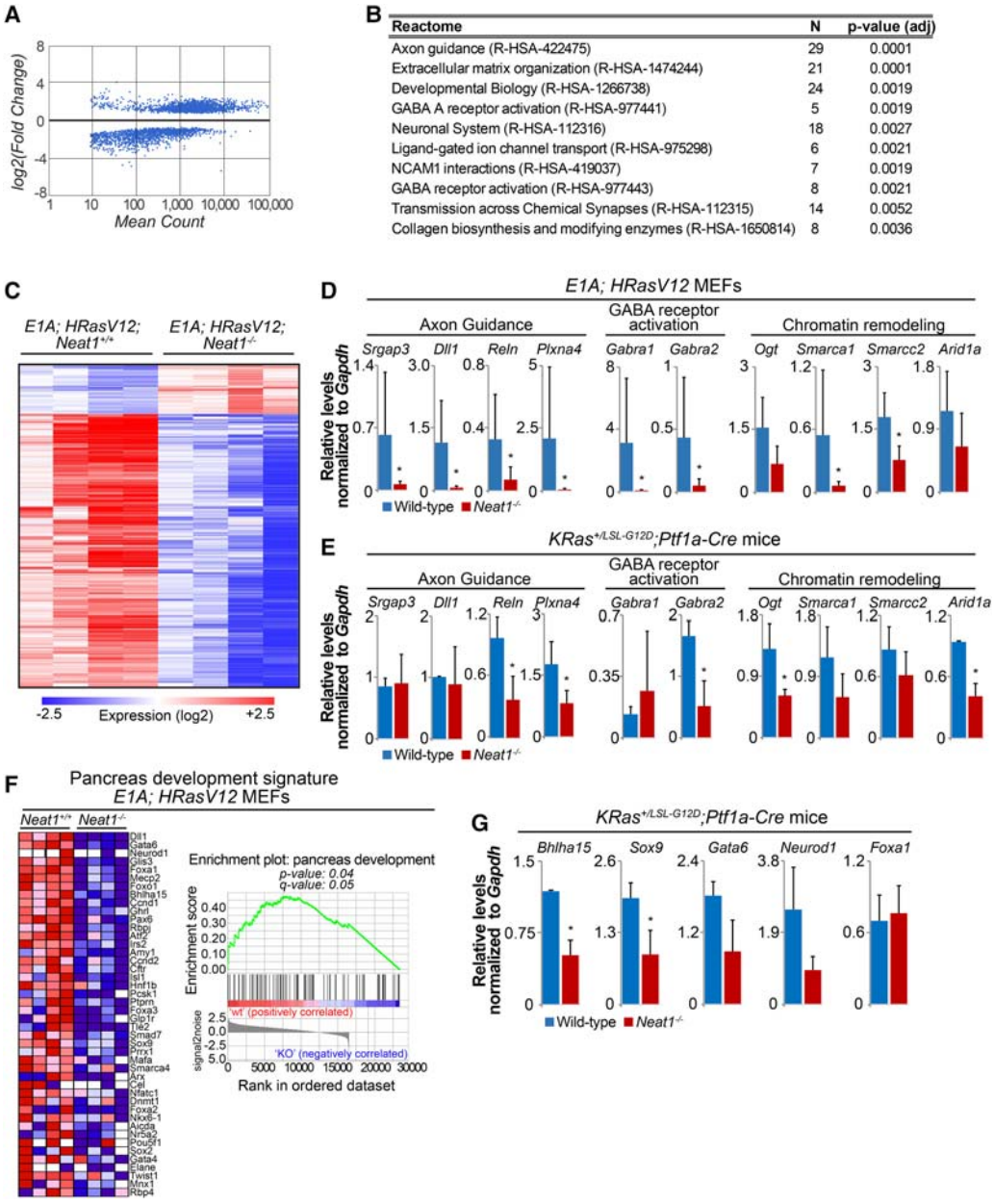

Reactome	N	p-value (adj)
Axon guidance (R-HSA-422475)	29	0.0001
Extracellular matrix organization (R-HSA-1474244)	21	0.0001
Developmental Biology (R-HSA-1266738)	24	0.0019
GABA A receptor activation (R-HSA-977441)	5	0.0019
Neuronal System (R-HSA-112316)	18	0.0027
Ligand-gated ion channel transport (R-HSA-975298)	6	0.0021
NCAM1 interactions (R-HSA-419037)	7	0.0019
GABA receptor activation (R-HSA-977443)	8	0.0021
Transmission across Chemical Synapses (R-HSA-112315)	14	0.0052
Collagen biosynthesis and modifying enzymes (R-HSA-1650814)	8	0.0036

Figure 7. *Neat1* deficiency triggers global gene expression program changes. (*A*) Scatter plot of the $\log_2$ (fold-change) versus the mean reads count per gene, generated using RNA-seq expression profiling data from *E1A;HRasV12;wild-type* and *E1A;HRasV12;Neat1*$^{-/-}$ MEFs. The dots represent differentially expressed genes according to DEseq2 analysis. (*B*) Table with Reactome categories found down-regulated in *E1A;HRasV12;Neat1*$^{-/-}$ MEFs. (*C*) Heat map representing the expression of the top differentially expressed genes in *E1A;HRasV12;wild-type* and *E1A;HRasV12;Neat1*$^{-/-}$ MEFs. (*D*) qRT–PCR analysis of genes involved in axon guidance, GABA receptor activation, and chromatin remodeling in *E1A;HRasV12;wild-type* and *E1A;HRasV12;Neat1*$^{-/-}$ MEFs, normalized to *Gapdh*. $n = 6$. (*E*) qRT–PCR analysis of expression of genes involved in axon guidance, GABA receptor activation, and chromatin remodeling in pancreata of *KRas*$^{+/LSL\text{-}G12D}$; *Ptf1a-Cre;Neat1*$^{+/+}$ and *KRas*$^{+/LSL\text{-}G12D}$*;Ptf1a-Cre;Neat1*$^{-/-}$ mice 7 d after cerulein treatment, normalized to *Gapdh*. $n = 2$. (*F*) Gene set enrichment analysis heat map of genes contributing to enrichment (*left*) and enrichment plot of pancreas development genes differentially expressed in *E1A;HRasV12;Neat1*$^{+/+}$ and *E1A;HRasV12;Neat1*$^{-/-}$ MEFs (*right*). False discovery rate is 0.052. (*G*) qRT–PCR analysis of pancreas development genes found differentially expressed in *E1A;HRasV12* MEFs in pancreata of *KRas*$^{+/LSL\text{-}G12D}$*;Ptf1a-Cre;Neat1*$^{+/+}$ and *KRas*$^{+/LSL\text{-}G12D}$*;Ptf1a-Cre;Neat1*$^{-/-}$ mice 7 d after cerulein treatment, normalized to *Gapdh*. (*) $P \leq 0.05$, based on the one-tailed unpaired Student's *t*-test.

networks involved in the differentiation and maintenance of pancreatic acinar and ductal cells, processes that could directly explain the susceptibility of $KRas^{G12D}$-expressing *Neat1*-deficient mice to the formation of different types of pancreatic preneoplastic lesions. Collectively, these findings suggest that the ability of *Neat1* to globally

regulate gene expression—with effects on diverse transcriptional programs—provides a potential mechanism for how *Neat1* acts to suppress transformation and tumor initiation.

Discussion

Here, we leveraged ChIP-seq and RNA-seq data from *p53* wild-type and $p53^{-/-}$ MEFs to identify p53-regulated ncRNAs that might help in understanding downstream components in p53 biological responses. We demonstrate that *Neat1/NEAT1* is a bona fide direct p53 target gene in diverse mouse and human cell types and that it is induced in response to different stress signals. Moreover, we queried its biological function downstream from p53 and provided the first evidence that *Neat1* is dispensable for p53-dependent cell cycle arrest or apoptosis responses to DNA damage. In dramatic contrast, however, we showed that *Neat1* does play a critical role in p53-dependent tumor suppression in oncogene-expressing fibroblast tumors and in suppression of pancreatic cancer initiation. Thus, our findings provide key genetic evidence that *Neat1* is a novel component of the p53 tumor suppression program.

Previous studies on *NEAT1* in cancer have focused primarily on *NEAT1* expression levels during the development of various types of human cancers. In some studies, *NEAT1* levels were found to increase during tumorigenesis, and high levels of *NEAT1* expression were associated with worse prognosis (Li et al. 2015; He et al. 2016; Ma et al. 2016; Wang et al. 2016). *NEAT1* can also promote cell survival and/or proliferation of human cancer cell lines, and *Neat1* acts as an oncogene in mice subjected to the DMBA-TPA skin carcinogenesis protocol (Adriaens et al. 2016). However, beyond the suggestion that *NEAT1* is an oncogene, other studies have suggested that *NEAT1* acts as a tumor suppressor in certain contexts. *NEAT1* is down-regulated in some cancers relative to normal tissue, augmented *NEAT1_2* levels were shown to predict better overall survival in colorectal cancer patients, and increased *NEAT1* levels were associated with enhanced apoptosis in irradiated chronic lymphocytic leukemia cells (Gibb et al. 2011; Blume et al. 2015; Wu et al. 2015). Moreover, *NEAT1_2* was found to inhibit cellular proliferation (Wu et al. 2015). These seemingly contradictory results may reflect cell type-specific roles for *NEAT1* in tumorigenesis. Importantly, these piecemeal and contradictory findings underscore the critical need for analysis of *Neat1* function in a genetically tractable animal model, such as *Neat1* knockout mice, to derive an unequivocal understanding of the role of *Neat1* in tumorigenesis.

Several molecular functions have been proposed for *NEAT1* that could relate to how it serves as a tumor suppressor. First, *NEAT1* is essential for the formation and maintenance of paraspeckles, (Clemson et al. 2009; Sasaki et al. 2009; Sunwoo et al. 2009), which have been suggested as sites of nuclear retention for adenosine-to-inosine (A-to-I) edited RNAs, thereby exerting an effect on gene expression at a post-transcriptional level (Prasanth et al. 2005; Chen and Carmichael 2009; Fox and Lamond 2010). Recent reports have also suggested that *NEAT1* may act at the post-transcriptional level by interacting with splicing factors and RNA 3′ end processing factors to modulate the proper maturation of precursor mRNAs (West et al. 2014). *NEAT1* can also regulate genes at the transcriptional level by sequestering transcriptional regulators into paraspeckles (Hirose et al. 2014) or binding the DNA of active genes (West et al. 2014) to increase active chromatin marks such as histone H3K4 trimethylation and histone H3K9 acetylation in these genes (Chakravarty et al. 2014), suggesting yet another pleotropic mechanism by which it could regulate the gene expression. Consistent with these transcriptional effects, the enhanced transformation and pancreatic neoplasia that we observed in the absence of *Neat1* are associated with altered gene expression programs in specific functional categories such as axon guidance, GABA A receptor activation, and chromatin remodeling. Interestingly, mutations in axon guidance genes were associated previously with pancreatic cancer in a study profiling the mutational landscape of this disease (Biankin et al. 2012). Indeed, some of the axon guidance genes with diminished expression upon *Neat1* deficiency have activities consistent with tumor suppression: *Srgap3*, which is involved in the inhibition of anchorage-independent growth; *Dll1*, which can reduce tumor growth and vascularization; Reln, which can restrain Ras and PI3K; and Plxna4, which is involved in the inhibition of bFGF and VEGF-induced cell proliferation (Kigel et al. 2011; Zhang et al. 2011; Lahoz and Hall 2013; Castellano et al. 2016). It will be interesting to reveal the transcriptional programs most critical for *NEAT1* activity in tumor suppression in more detail in future studies.

The mechanisms underlying *Neat1/NEAT1* function described above may also provide key insights into how it might modulate cellular responses during tumor suppression. *Neat1/NEAT1* has been shown previously to control several aspects of cell behavior by enhancing or decreasing cell division, inhibiting cell death, and increasing migration (Chakravarty et al. 2014; Chen et al. 2015; Choudhry et al. 2015; Wu et al. 2015; Ma et al. 2016; Wang et al. 2016). Our findings in the pancreatic cancer model support the notion that *Neat1* inhibits cell proliferation. In addition, the observation that *Neat1/NEAT1* levels increase during differentiation of a variety of cell types, including ESCs, muscle cells, neuronal cells, and glial cells, suggests that *NEAT1* may play a role in cellular differentiation (Lehnert et al. 2007; Chen and Carmichael 2009; Sunwoo et al. 2009; Mercer et al. 2010; Zeng et al. 2014). Moreover, studies of *Neat1*-null mice have shown that *Neat1* is required for proper corpus luteum differentiation and mammary gland development (Nakagawa et al. 2014; Standaert et al. 2014). Consistent with a role in regulating differentiation is our observation that *Neat1* deficiency in $Kras^{G12D}$-expressing acini triggers increased ADM, a dedifferentiation event through which terminally differentiated acinar cells reprogram into ductal cells and then PanINs, leading ultimately to PDAC development (Kopp et al. 2012). In addition, we found that $Kras^{G12D}$-expressing *Neat1*-deficient mice are prone to develop cystic

lesions, suggesting that *Neat1* could also be acting in more than one way to limit pancreatic neoplasia. Ductal cells undergo a dedifferentiation process to become IPMN lesions (Roy et al. 2015), and our results thus suggest that *Neat1* is also involved in the maintenance of terminally differentiated ductal cells in the context of oncogenic Kras. The decreased expression of pancreatic differentiation genes observed upon *Neat1* loss support an important role for *Neat1* in differentiation in the pancreas. Interestingly, *Neat1*$^{-/-}$ mice in the context of wild-type KRas are not reported to develop cancer, and we similarly did not detect any noticeable developmental defects or pancreas abnormalities of *Neat1*$^{-/-}$ mice (Supplemental Fig. S8), reinforcing the idea that *Neat1* tumor suppressor activities are triggered only upon oncogenic stress. Collectively, our findings suggest that *Neat1* function in differentiation could be the basis for its activity as a suppressor of transformation and pancreatic neoplasia.

Despite the unequivocal importance of p53 in tumor suppression, the mechanisms through which it suppresses cancer development remain elusive. Recent studies have suggested that the best-characterized p53 functions— inducing cell cycle arrest or apoptosis in response to genotoxic stresses—as well as the well-studied p53 target genes involved in these responses (*p21*, *Noxa*, and *Puma*) are dispensable for tumor suppression (Brady et al. 2011; Li et al. 2012; Valente et al. 2013). New strategies are therefore needed to elucidate the molecular underpinnings of p53 tumor suppressor function. Here, the use of genomic approaches such as ChIP-seq and RNA-seq has helped to greatly expand the repertoire of genes known to be directly regulated by p53. Our discovery that *Neat1/NEAT1* is a conserved p53-inducible lincRNA with a critical role in p53-dependent transformation suppression provides a key piece to the p53 tumor suppression puzzle. Understanding the cellular and molecular basis for how *NEAT1* acts as a tumor suppressor will ultimately greatly expand our understanding of p53-mediated tumor suppression.

Materials and methods

Cell culture experiments

MEFs, colorectal cancer cells (HCT116), and pancreatic cancer cells were cultured in DMEM containing 10% FBS. Primary human fibroblasts are originally from Coriell Cell Repository and were cultured in DMEM containing 15% FBS. Human ESCs H9 (Wicell) and LSJ2 (Stanford) were maintained as described (Conklin et al. 2012). Mouse ESCs were cultured together with irradiated feeders in DMEM supplemented with 20% stem cell certified FBS, 10% NEAA, LIF, and β-mercaptoethanol. Doxorubicin (Sigma) treatment was at 0.2 μg/mL, and Nutlin-3a (Sigma-Aldrich) was at 10 μM. UV-C treatment was at 20 J/m^2, and ionizing radiation dose was 5 Gy of γ radiation. Lentiviral infections for gene silencing or overexpression were performed as described (Brady et al. 2011). siRNA transfection using sequences against *p53* (Dharmacon, M-003329-03) or *NEAT1* were performed using Dharmafect 4 (Dharmacon) according to the manufacture's protocol, and siGENOME nontargeting siRNA pools (Dharmacon, D-001206-14) were used as a control. For clonogenic assays in which *Neat1* or *p53* was overexpressed, *E1A;HRasV12*; *p53*$^{-/-}$ MEFs were transduced with pLEX MCS-empty (negative control), pLEX MCS-p53 (positive control), or pLEX MCS-*Neat1*.

Cell cycle arrest and apoptosis assays

MEFs were irradiated, 5-ethynyl-2′-deoxyuridine (EdU)-pulsed after 14 h for 4 h, and processed using the Click-iT EdU Alexa fluor 488 imaging kit (ThermoFisher Scientific) according to the manufacturer's protocol. For apoptosis experiments, *E1A;HRasV12* MEFs were treated with doxorubicin for 12 or 24 h and stained with Annexin V FITC (Invitrogen) and PI, following the manufacturer's protocol. Both cell cycle and apoptosis experiments were assessed by flow cytometry.

Clonogenic assays, anchorage-independent growth assays, and subcutaneous tumor studies

For the clonogenic assays, *E1A;HRasV12* MEFs were plated in triplicate on six-well plates at 150 cells per well and left to grow for ~12 d. Cells were fixed with 10% formalin and stained with 0.1% crystal violet. Anchorage-independent growth assays were performed as described previously (Kenzelmann Broz et al. 2013). Plates were scanned, and colony number quantification was performed manually for clonogenic assays, while OpenCFU (Geissmann 2013) was used to quantify the scanned images of wells from the anchorage-independent growth assays. Subcutaneous tumor studies were performed as described (Brady et al. 2011).

RNA-seq and data sets

Total RNA was extracted from wild-type and *Neat1*$^{-/-}$ *E1A;HRasV12* MEFs using the Qiagen RNeasy mini extraction kit (Qiagen) according to the manufacturer's protocol. RNA-seq libraries were generated using the Illumina TruSeq kit (version 2) following the manufacturer's instructions. The libraries were sequenced on a HiSeq 4000 system (Illumina), and the RNA-seq reads were analyzed with Basespace's RNA Express pipeline (RNA Express Legacy version: 1.0.0), which encompasses alignment using the STAR aligner (Dobin et al. 2013) and differential expression analysis using DESEQ2 (Love et al. 2014). Differentially regulated genes were also analyzed using Enrichr (Chen et al. 2013; Kuleshov et al. 2016) to detect which biological pathways are being altered upon *Neat1* loss. GSEA was used to test whether *Neat1* deficiency impacts the expression of genes involved in pancreas development (Subramanian et al. 2005). A pancreas development signature was generated based on a previously published study (Arda et al. 2013). The RNA-seq data generated by this work is available in the Gene Expression Omnibus (GEO) database under accession number GSE100098. For the identification of *NEAT1/Neat1* as a p53 target gene, previously generated mouse ChIP-seq and RNA-seq data sets (GSE46240) as well as a human p53 ChIP-seq data set (GSE55727) were used.

qRT–PCR, RNA-FISH, and Northern blot analysis

RNA was isolated using Trizol (Invitrogen) and reverse-transcribed using MMLV reverse transcriptase (Invitrogen) and random primers. qPCR was performed with Power SYBR Green PCR master mix (Thermo Fisher) and a 7900HT Fast real-time PCR machine (Applied Biosystems). A standard curve was used to quantify the samples. ChIP-qPCR was performed as described (Kenzelmann Broz et al. 2013). Primer sequences for qRT–PCR and ChIP-qPCR are listed in Supplemental Table S1. RNA-FISH was performed using Stellaris RNA-FISH complex probe sets (Biosearch Technologies) according to the manufacturer's protocol. The mouse *Neat1* probe set was Quasar 570-labeled, while the

human *NEAT1* probe set was FAM (6-carboxyfluorescein)-labeled. Double staining with Sfpq was performed using a rabbit polyclonal anti-Sfpq antibody (1:200; Bethyl Laboratories). Northern blotting was performed as described (Johnson et al. 2005).

Mouse models for pancreatic cancer

Pancreatitis was triggered by treating 8-wk-old *KRas*$^{+/LSL\text{-}G12D}$; *Ptf1a-Cre*, *KRas*$^{+/LSL\text{-}G12D}$;*Ptf1a-Cre*;*Neat1*$^{+/-}$, and *KRas*$^{+/LSL\text{-}G12D}$;*Ptf1a-Cre*;*Neat1*$^{-/-}$ mice with eight hourly intraperitoneal injections of cerulein (100 µg per kilogram of body weight; Sigma-Aldrich) over 2 d, as described previously (Jensen et al. 2005). Mice were sacrificed 7 d after cerulein treatment, and the pancreata were analyzed by different histological parameters. Spontaneous transformation was also assessed in mice aged for 5 mo. Both groups were evaluated by a trained pathologist specializing in pancreatic cancer. Mice were on a 129/Sv and C57BL/6 mixed background.

Histology and immunohistochemistry

Tissue specimen processing, sectioning, and H&E staining were performed using standard protocols. Immunohistochemistry was performed using the VectaStain Elite ABC kit (Vector Laboratories) according to the manufacturer's protocol. The antibodies used were mouse anti-MUC5AC (1:500; ThermoFisher), mouse anti-Ki67 (1:100; BD Pharmingen), rat anti-Ck19 (1:750; University of Iowa), and goat anti-amylase (1:100; Santa Cruz Biotechnology). The sections were counterstained with hematoxylin or Alcian blue/nuclear fast red using the NovaUltra Alcian blue stain kit (IHC World) according to the manufacturer's instructions. For Ck19 and amylase staining, the sections were stained using anti-goat Alexa 488 (1:200; Invitrogen) and anti-rat Alexa 594 (1:200; Invitrogen) and counterstained with DAPI. Pictures were taken using a Leica microscope and/or with a NanoZoomer 2.0-RS slide scanner (Hamamatsu). Analysis of the PanIN and mucinous cystic lesion areas and Ki67 staining was performed using ImageJ. To simulate the size criterion used to diagnose IPMNs in humans, we also used a size criterion (diameter ≥280) to call cystic lesions/IPMNs. This size was based on the ability to distinguish large cystic lesions from PanIN lesions. Further classification of these lesions was performed based on their lining using H&E and Muc5ac staining.

Acknowledgments

We thank J.C. Marine, B.M. Flowers, and A. Kaiser for critical discussions and reading of the manuscript. We thank P. Chu of the Stanford Comparative Medicine Histology Research Core Laboratory for technical assistance with tissue processing, sectioning, and staining; A. Fox and G. Pierron for plasmids; N. Bardeesy for p53-deficient pancreatic cancer cells; J.C. Marine for *Neat1* knockout MEFs; and E. Majunder for technical assistance. This work was supported by funding from the National Institutes of Health (R01 ES020260 to J.R. and L.D.A., and R35 CA197591 to L.D.A.) and the Lustgarten Foundation (J.S.).

References

Adriaens C, Standaert L, Barra J, Latil M, Verfaillie A, Kalev P, Boeckx B, Wijnhoven PWG, Radaelli E, Vermi W, et al. 2016. p53 induces formation of NEAT1 lncRNA-containing paraspeckles that modulate replication stress response and chemosensitivity. *Nat Med* **22:** 861–868.

Amankwah EK, Thompson RC, Nabors LB, Olson JJ, Browning JE, Madden MH, Egan KM. 2013. SWI/SNF gene variants and glioma risk and outcome. *Cancer Epidemiol* **37:** 162–165.

Arda HE, Benitez CM, Kim SK. 2013. Gene regulatory networks governing pancreas development. *Dev Cell* **25:** 5–13.

Balakrishnan A, Penachioni JY, Lamba S, Bleeker FE, Zanon C, Rodolfo M, Vallacchi V, Scarpa A, Felicioni L, Buck M, et al. 2009. Molecular profiling of the 'plexinome' in melanoma and pancreatic cancer. *Hum Mutat* **30:** 1167–1174.

Biankin AV, Waddell N, Kassahn KS, Gingras M-C, Muthuswamy LB, Johns AL, Miller DK, Wilson PJ, Patch A-M, Wu J, et al. 2012. Pancreatic cancer genomes reveal aberrations in axon guidance pathway genes. *Nature* **491:** 399–405.

Bieging KT, Mello SS, Attardi LD. 2014. Unravelling mechanisms of p53-mediated tumour suppression. *Nat Rev Cancer* **14:** 359–370.

Blume CJ, Hotz-Wagenblatt A, Hullein J, Sellner L, Jethwa A, Stolz T, Slabicki M, Lee K, Sharathchandra A, Benner A, et al. 2015. p53-dependent non-coding RNA networks in chronic lymphocytic leukemia. *Leukemia* **29:** 2015–2023.

Botcheva K, McCorkle SR, McCombie WR, Dunn JJ, Anderson CW. 2011. Distinct p53 genomic binding patterns in normal and cancer-derived human cells. *Cell Cycle* **10:** 4237–4249.

Brady CA, Attardi LD. 2010. p53 at a glance. *J Cell Sci* **123:** 2527–2532.

Brady CA, Jiang D, Mello SS, Johnson TM, Jarvis LA, Kozak MM, Broz DK, Basak S, Park EJ, McLaughlin ME, et al. 2011. Distinct p53 transcriptional programs dictate acute DNA-damage responses and tumor suppression. *Cell* **145:** 571–583.

Castellano E, Molina-Arcas M, Krygowska AA, East P, Warne P, Nicol A, Downward J. 2016. RAS signalling through PI3-kinase controls cell migration via modulation of Reelin expression. *Nat Commun* **7:** 11245.

Chakravarty D, Sboner A, Nair SS, Giannopoulou E, Li R, Hennig S, Mosquera JM, Pauwels J, Park K, Kossai M, et al. 2014. The oestrogen receptor α-regulated lncRNA NEAT1 is a critical modulator of prostate cancer. *Nat Commun* **5:** 5383.

Chedotal A, Kerjan G, Moreau-Fauvarque C. 2005. The brain within the tumor: new roles for axon guidance molecules in cancers. *Cell Death Differ* **12:** 1044–1056.

Chen L-L, Carmichael GG. 2009. Altered nuclear retention of mRNAs containing inverted repeats in human embryonic stem cells: functional role of a nuclear noncoding RNA. *Mol Cell* **35:** 467–478.

Chen EY, Tan CM, Kou Y, Duan Q, Wang Z, Meirelles GV, Clark NR, Ma'ayan A. 2013. Enrichr: interactive and collaborative HTML5 gene list enrichment analysis tool. *BMC Bioinformatics* **14:** 128.

Chen X, Kong J, Ma Z, Gao S, Feng X. 2015. Up regulation of the long non-coding RNA NEAT1 promotes esophageal squamous cell carcinoma cell progression and correlates with poor prognosis. *Am J Cancer Res* **5:** 2808–2815.

Choi YJ, Lin C-P, Ho JJ, He X, Okada N, Bu P, Zhong Y, Kim SY, Bennett MJ, Chen C, et al. 2011. miR-34 miRNAs provide a barrier for somatic cell reprogramming. *Nat Cell Biol* **13:** 1353–1360.

Choudhry H, Albukhari A, Morotti M, Haider S, Moralli D, Smythies J, Schödel J, Green CM, Camps C, Buffa F, et al. 2015. Tumor hypoxia induces nuclear paraspeckle formation through HIF-2α dependent transcriptional activation of NEAT1 leading to cancer cell survival. *Oncogene* **34:** 4482–4490.

Clemson CM, Hutchinson JN, Sara SA, Ensminger AW, Fox AH, Chess A, Lawrence JB. 2009. An architectural role for a nuclear noncoding RNA: NEAT1 RNA is essential for the structure of paraspeckles. *Molecular Cell* **33:** 717–726.

Conklin JF, Baker J, Sage J. 2012. The RB family is required for the self-renewal and survival of human embryonic stem cells. *Nat Commun* **3:** 1244.

Dallol A, Morton D, Maher ER, Latif F. 2003. SLIT2 axon guidance molecule is frequently inactivated in colorectal cancer and suppresses growth of colorectal carcinoma cells. *Cancer Res* **63:** 1054–1058.

Direnzo D, Hess DA, Damsz B, Hallett JE, Marshall B, Goswami C, Liu Y, Deering T, Macdonald RJ, Konieczny SF. 2012. Induced Mist1 expression promotes remodeling of mouse pancreatic acinar cells. *Gastroenterology* **143:** 469–480.

Dobin A, Davis CA, Schlesinger F, Drenkow J, Zaleski C, Jha S, Batut P, Chaisson M, Gingeras TR. 2013. STAR: ultrafast universal RNA-seq aligner. *Bioinformatics* **29:** 15–21.

Fox AH, Lamond AI. 2010. Paraspeckles. *Cold Spring Harb Perspect Biol* **2:** a000687.

Geissmann Q. 2013. OpenCFU, a new free and open-source software to count cell colonies and other circular objects. *PLoS One* **8:** e54072.

Gibb EA, Vucic EA, Enfield KSS, Stewart GL, Lonergan KM, Kennett JY, Becker-Santos DD, MacAulay CE, Lam S, Brown CJ, et al. 2011. Human cancer long non-coding RNA transcriptomes. *PLoS One* **6:** e25915.

Göhrig A, Detjen KM, Hilfenhaus G, Körner JL, Welzel M, Arsenic R, Schmuck R, Bahra M, Wu JY, Wiedenmann B. 2014. Axon guidance factor SLIT2 inhibits neural invasion and metastasis in pancreatic cancer. *Cancer Res* **74:** 1529–1540.

Guerra C, Schuhmacher AJ, Cañamero M, Grippo PJ, Verdaguer L, Pérez-Gallego L, Dubus P, Sandgren EP, Barbacid M. 2007. Chronic pancreatitis is essential for induction of pancreatic ductal adenocarcinoma by K-Ras oncogenes in adult mice. *Cancer Cell* **11:** 291–302.

Guerra C, Collado M, Navas C, Schuhmacher Alberto J, Hernández-Porras I, Cañamero M, Rodriguez-Justo M, Serrano M, Barbacid M. 2011. Pancreatitis-induced inflammation contributes to pancreatic cancer by inhibiting oncogene-induced senescence. *Cancer Cell* **19:** 728–739.

He C, Jiang B, Ma J, Li Q. 2016. Aberrant NEAT1 expression is associated with clinical outcome in high grade glioma patients. *APMIS* **124:** 169–174.

Hirose T, Virnicchi G, Tanigawa A, Naganuma T, Li R, Kimura H, Yokoi T, Nakagawa S, Bénard M, Fox AH, et al. 2014. NEAT1 long noncoding RNA regulates transcription via protein sequestration within subnuclear bodies. *Mol Biol Cell* **25:** 169–183.

Huarte M, Guttman M, Feldser D, Garber M, Koziol MJ, Kenzelmann-Broz D, Khalil AM, Zuk O, Amit I, Rabani M, et al. 2010. A large intergenic noncoding RNA induced by p53 mediates global gene repression in the p53 response. *Cell* **142:** 409–419.

Hung T, Wang Y, Lin MF, Koegel AK, Kotake Y, Grant GD, Horlings HM, Shah N, Umbricht C, Wang P, et al. 2011. Extensive and coordinated transcription of noncoding RNAs within cell-cycle promoters. *Nat Genet* **43:** 621–629.

Hutchinson JN, Ensminger AW, Clemson CM, Lynch CR, Lawrence JB, Chess A. 2007. A screen for nuclear transcripts identifies two linked noncoding RNAs associated with SC35 splicing domains. *BMC Genomics* **8:** 39.

Jensen JN, Cameron E, Garay MVR, Starkey TW, Gianani R, Jensen J. 2005. Recapitulation of elements of embryonic development in adult mouse pancreatic regeneration. *Gastroenterology* **128:** 728–741.

Johnson TM, Hammond EM, Giaccia A, Attardi LD. 2005. The p53QS transactivation-deficient mutant shows stress-specific apoptotic activity and induces embryonic lethality. *Nat Genet* **37:** 145–152.

Kenzelmann Broz D, Spano Mello S, Bieging KT, Jiang D, Dusek RL, Brady CA, Sidow A, Attardi LD. 2013. Global genomic profiling reveals an extensive p53-regulated autophagy program contributing to key p53 responses. *Genes Dev* **27:** 1016–1031.

Kigel B, Rabinowicz N, Varshavsky A, Kessler O, Neufeld G. 2011. Plexin-A4 promotes tumor progression and tumor angiogenesis by enhancement of VEGF and bFGF signaling. *Blood* **118:** 4285–4296.

Kopp Janel L, von Figura G, Mayes E, Liu F-F, Dubois Claire L, Morris Iv John P, Pan Fong C, Akiyama H, Wright Christopher VE, Jensen K, et al. 2012. Identification of Sox9-dependent acinar-to-ductal reprogramming as the principal mechanism for initiation of pancreatic ductal adenocarcinoma. *Cancer Cell* **22:** 737–750.

Krizhanovsky V, Lowe SW. 2009. Stem cells: the promises and perils of p53. *Nature* **460:** 1085–1086.

Kruiswijk F, Labuschagne CF, Vousden KH. 2015. p53 in survival, death and metabolic health: a lifeguard with a licence to kill. *Nat Rev Mol Cell Biol* **16:** 393–405.

Kuleshov MV, Jones MR, Rouillard AD, Fernandez NF, Duan Q, Wang Z, Koplev S, Jenkins SL, Jagodnik KM, Lachmann A, et al. 2016. Enrichr: a comprehensive gene set enrichment analysis Web server 2016 update. *Nucleic Acids Res* **44:** W90–W97.

Lahoz A, Hall A. 2013. A tumor suppressor role for srGAP3 in mammary epithelial cells. *Oncogene* **32:** 4854–4860.

Lehnert SA, Reverter A, Byrne KA, Wang Y, Nattrass GS, Hudson NJ, Greenwood PL. 2007. Gene expression studies of developing bovine longissimusmuscle from two different beef cattle breeds. *BMC Dev Biol* **7:** 1–13.

Léveillé N, Melo CA, Rooijers K, Díaz-Lagares A, Melo SA, Korkmaz G, Lopes R, Moqadam FA, Maia AR, Wijchers PJ, et al. 2015. Genome-wide profiling of p53-regulated enhancer RNAs uncovers a subset of enhancers controlled by a lncRNA. *Nat Commun* **6:** 6520.

Li T, Kon N, Jiang L, Tan M, Ludwig T, Zhao Y, Baer R, Gu W. 2012. Tumor suppression in the absence of p53-mediated cell-cycle arrest, apoptosis, and senescence. *Cell* **149:** 1269–1283.

Li Y, Li Y, Chen W, He F, Tan Z, Zheng J, Wang W, Zhao Q, Li J. 2015. NEAT expression is associated with tumor recurrence and unfavorable prognosis in colorectal cancer. *Oncotarget* **6:** 27641–27650.

Liu Q, Huang J, Zhou N, Zhang Z, Zhang A, Lu Z, Wu F, Mo Y-Y. 2013. LncRNA loc285194 is a p53-regulated tumor suppressor. *Nucleic Acids Res* **41:** 4976–4987.

Love MI, Huber W, Anders S. 2014. Moderated estimation of fold change and dispersion for RNA-seq data with DESeq2. *Genome Biol* **15:** 550.

Lowe SW, Schmitt EM, Smith SW, Osborne BA, Jacks T. 1993. p53 is required for radiation induced apoptosis in mouse thymocytes. *Nature* **362:** 847–849.

Ma Y, Liu L, Yan F, Wei W, Deng J, Sun J. 2016. Enhanced expression of long non-coding RNA NEAT1 is associated with the progression of gastric adenocarcinomas. *World J Surg Oncol* **14:** 1–6.

Martinelli P, Canamero M, del Pozo N, Madriles F, Zapata A, Real FX. 2013. Gata6 is required for complete acinar differentiation and maintenance of the exocrine pancreas in adult mice. *Gut* **62:** 1481–1488.

Matthaei H, Schulick RD, Hruban RH, Maitra A. 2011. Cystic precursors to invasive pancreatic cancer. *Nat Rev Gastroenterol Hepatol* **8:** 141–150.

Mercer TR, Qureshi IA, Gokhan S, Dinger ME, Li G, Mattick JS, Mehler MF. 2010. Long noncoding RNAs in neuronal-glial fate specification and oligodendrocyte lineage maturation. *BMC Neurosci* **11:** 1–15.

Mi Je E, Gwak M, Oh H, Ryoung Choi M, Jin Choi Y, Lee SH, Jin Yoo N. 2013. Frameshift mutations of axon guidance genes ROBO1 and ROBO2 in gastric and colorectal cancers with microsatellite instability. *Pathology* **45:** 645–650.

Morris JP, Cano DA, Sekine S, Wang SC, Hebrok M. 2010. β-Catenin blocks Kras-dependent reprogramming of acini into pancreatic cancer precursor lesions in mice. *J Clin Invest* **120:** 508–520.

Naganuma T, Hirose T. 2013. Paraspeckle formation during the biogenesis of long non-coding RNAs. *RNA Biol* **10:** 456–461.

Nakagawa S, Naganuma T, Shioi G, Hirose T. 2011. Paraspeckles are subpopulation-specific nuclear bodies that are not essential in mice. *J Cell Biol* **193:** 31–39.

Nakagawa S, Shimada M, Yanaka K, Mito M, Arai T, Takahashi E, Fujita Y, Fujimori T, Standaert L, Marine J-C, et al. 2014. The lncRNA Neat1 is required for corpus luteum formation and the establishment of pregnancy in a subpopulation of mice. *Development* **141:** 4618–4627.

Okada N, Lin C-P, Ribeiro MC, Biton A, Lai G, He X, Bu P, Vogel H, Jablons DM, Keller AC, et al. 2014. A positive feedback between p53 and miR-34 miRNAs mediates tumor suppression. *Genes Dev* **28:** 438–450.

Olivier M, Hollstein M, Hainaut P. 2010. TP53 mutations in human cancers: origins, consequences, and clinical use. *Cold Spring Harb Perspect Biol* **2:** a001008.

Prasanth KV, Prasanth SG, Xuan Z, Hearn S, Freier SM, Bennett CF, Zhang MQ, Spector DL. 2005. Regulating gene expression through RNA nuclear retention. *Cell* **123:** 249–263.

Roy N, Malik S, Villanueva KE, Urano A, Lu X, Von Figura G, Seeley ES, Dawson DW, Collisson EA, Hebrok M. 2015. Brg1 promotes both tumor-suppressive and oncogenic activities at distinct stages of pancreatic cancer formation. *Genes Dev* **29:** 658–671.

Sánchez Y, Segura V, Marín-Béjar O, Athie A, Marchese FP, González J, Bujanda L, Guo S, Matheu A, Huarte M. 2014. Genome-wide analysis of the human p53 transcriptional network unveils a lncRNA tumour suppressor signature. *Nat Commun* **5:** 5812.

Sasaki YTF, Ideue T, Sano M, Mituyama T, Hirose T. 2009. MENε/β noncoding RNAs are essential for structural integrity of nuclear paraspeckles. *Proc Natl Acad Sci* **106:** 2525–2530.

Sato N, Fukushima N, Chang R, Matsubayashi H, Goggins M. 2006. Differential and epigenetic gene expression profiling identifies frequent disruption of the RELN pathway in pancreatic cancers. *Gastroenterology* **130:** 548–565.

Schmitt AM, Chang HY. 2016. Long noncoding RNAs in cancer pathways. *Cancer Cell* **29:** 452–463.

Schmitt AM, Garcia JT, Hung T, Flynn RA, Shen Y, Qu K, Payumo AY, Peres-da-Silva A, Broz DK, Baum R, et al. 2016. An inducible long noncoding RNA amplifies DNA damage signaling. *Nat Genet* **48:** 1370–1376.

Seymour PA. 2014. Sox9: a master regulator of the pancreatic program. *Rev Diabet Stud* **11:** 51–83.

Shi G, Zhu L, Sun Y, Bettencourt R, Damsz B, Hruban RH, Konieczny SF. 2009. Loss of the acinar-restricted transcription factor Mist1 accelerates Kras-induced pancreatic intraepithelial neoplasia. *Gastroenterology* **136:** 1368–1378.

Standaert L, Adriaens C, Radaelli E, Keymeulen A, Blanpain C, Hirose T. 2014. The long noncoding RNA Neat1 is required for mammary gland development and lactation. *RNA* **20:** 1844–1849.

Subramanian A, Tamayo P, Mootha VK, Mukherjee S, Ebert BL, Gillette MA, Paulovich A, Pomeroy SL, Golub TR, Lander ES, et al. 2005. Gene set enrichment analysis: a knowledge-based approach for interpreting genome-wide expression profiles. *Proc Natl Acad Sci* **102:** 15545–15550.

Sunwoo H, Dinger ME, Wilusz JE, Amaral PP, Mattick JS, Spector DL. 2009. MENε/β nuclear-retained non-coding RNAs are up-regulated upon muscle differentiation and are essential components of paraspeckles. *Genome Res* **19:** 347–359.

Takeshima H, Niwa T, Takahashi T, Wakabayashi M, Yamashita S, Ando T, Inagawa Y, Taniguchi H, Katai H, Sugiyama T, et al. 2015. Frequent involvement of chromatin remodeler alterations in gastric field cancerization. *Cancer Lett* **357:** 328–338.

Tanaka T, Kuroki T, Adachi T, Ono S, Hirabaru M, Soyama A, Kitasato A, Takatsuki M, Hayashi T, Eguchi S. 2013. Evaluation of SOX9 expression in pancreatic ductal adenocarcinoma and intraductal papillary mucinous neoplasm. *Pancreas* **42:** 488–493.

Truitt ML, Ruggero D. 2016. New frontiers in translational control of the cancer genome. *Nat Rev Cancer* **16:** 288–304.

Valente Liz J, Gray Daniel HD, Michalak Ewa M, Pinon-Hofbauer J, Egle A, Scott Clare L, Janic A, Strasser A. 2013. p53 efficiently suppresses tumor development in the complete absence of its cell-cycle inhibitory and proapoptotic effectors p21, Puma, and Noxa. *Cell Rep* **3:** 1339–1345.

Vassilev LT, Vu BT, Graves B, Carvajal D, Podlaski F, Filipovic Z, Kong N, Kammlott U, Lukacs C, Klein C, et al. 2004. In vivo activation of the p53 pathway by small-molecule antagonists of MDM2. *Science* **303:** 844–848.

von Figura G, Fukuda A, Roy N, Liku ME, Morris Iv JP, Kim GE, Russ HA, Firpo MA, Mulvihill SJ, Dawson DW, et al. 2014. The chromatin regulator Brg1 suppresses formation of intraductal papillary mucinous neoplasm and pancreatic ductal adenocarcinoma. *Nat Cell Biol* **16:** 255–267.

Vousden KH, Prives C. 2009. Blinded by the light: the growing complexity of p53. *Cell* **137:** 413–431.

Wang P, Wu T, Zhou H, Jin Q, He G, Yu H, Xuan L, Wang X, Tian L, Sun Y, et al. 2016. Long noncoding RNA NEAT1 promotes laryngeal squamous cell cancer through regulating miR-107/CDK6 pathway. *J Exp Clin Cancer Res* **35:** 1–11.

Weissman B, Knudsen KE. 2009. Hijacking the chromatin remodeling machinery: impact of SWI/SNF perturbations in cancer. *Cancer Res* **69:** 8223–8230.

West JA, Davis CP, Sunwoo H, Simon MD, Sadreyev RI, Wang PI, Tolstorukov MY, Kingston RE. 2014. The long noncoding RNAs NEAT1 and MALAT1 bind active chromatin sites. *Mol Cell* **55:** 791–802.

Wilson BG, Roberts CWM. 2011. SWI/SNF nucleosome remodellers and cancer. *Nat Rev Cancer* **11:** 481–492.

Wu Y, Yang L, Zhao J, Li C, Nie J, Liu F, Zhuo C, Zheng Y, Li B, Wang Z, et al. 2015. Nuclear-enriched abundant transcript 1 as a diagnostic and prognostic biomarker in colorectal cancer. *Mol Cancer* **14:** 1–12.

Younger ST, Kenzelmann-Broz D, Jung H, Attardi LD, Rinn JL. 2015. Integrative genomic analysis reveals widespread enhancer regulation by p53 in response to DNA damage. *Nucleic Acids Res* **43:** 4447–4462.

Zeng C, Xu Y, Xu L, Yu X, Cheng J, Yang L, Chen S, Li Y. 2014. Inhibition of long non-coding RNA NEAT1 impairs myeloid differentiation in acute promyelocytic leukemia cells. *BMC Cancer* **14:** 1–7.

Zhang JP, Qin HY, Wang L, Liang L, Zhao XC, Cai WX, Wei YN, Wang CM, Han H. 2011. Overexpression of Notch ligand Dll1 in B16 melanoma cells leads to reduced tumor growth due to attenuated vascularization. *Cancer Lett* **309:** 220–227.

Zhu L, Shi G, Schmidt CM, Hruban RH, Konieczny SF. 2007. Acinar cells contribute to the molecular heterogeneity of pancreatic intraepithelial neoplasia. *Am J Pathol* **171:** 263–273.